A non-linear model for the fatigue assessment of notched components under fatigue loadings

P. Livieri*, E. Salvati**, R. Tovo*

*Department of Engineering, University of Ferrara, Via Saragat 1, 44122 Ferrara (Italy)
** Department of Engineering Science, University of Oxford, Parks Road, Oxford, OX1 3PJ, (UK)

Abstract

This paper presents a general theory for the estimations of an entire fatigue curve in ductile materials based on the implicit gradient approach. In order to modify the slope of the Woehler curves, the material was considered non-linear. The average stress of the hysteresis loop was taken into account by means of Walker's model. Subsequently, the implicit gradient method was adopted for the numerical evaluation of the effective stress and strain at low- and medium-cycle fatigue life and was then related to the fatigue strength of the material. The characteristic length, relating to the fatigue behaviour of the material, was considered constant for the fatigue lifetime. In order to confirm the proposed method, new experimental data were obtained, relating to axisymmetric notched specimens loaded with nominal stress ratio R=-1 and R=0. In terms of the effective strain amplitude, evaluated by means of the implicit gradient approach, the different Woehler curves of notched specimens were summarised in a unique fatigue curve as a function of Walker's cycle parameter.

Keywords: notches, implicit gradient, non-linear behaviour, equivalent stress

Corresponding author:
Paolo Livieri, e-mail: paolo.livieri@unife.it

Nomenclature

b = exponent for the elastic strain of the Manson-Coffin stain–life curve

b_w = exponent for a Walker stain–life curve

$\bar{c}$ = characteristic material parameter

c = exponent for the elastic strain of the Manson-Coffin stain–life curve

c_w = exponent for a Walker stain–life curve

E = elastic modulus

k = strength coefficient monotonic stress-strain curve

k' = strength coefficient cyclic stress-strain curve

K_t = stress concentration factor

n = hardening exponent monotonic stress-strain curve

n' = hardening exponent cyclic stress-strain curve

N_f = fatigue life; cycles to failure

N_i = cycle number for the intersection point for a two-segment stress–life curve

N_{fw}= equivalent value of N_f from Walker's method; Walker's equivalent life

R = stress ratio, R = σmin/σmax

$\Delta\varepsilon$ = strain range, $\Delta\varepsilon = 2\varepsilon_a$

$\Delta\sigma$ = stress range, $\Delta\sigma = 2\sigma_a$

ε_a = strain amplitude

ε_{pa} = plastic strain amplitude

γ = exponent for Walker's method

σ_a = stress amplitude

σ_m = mean stress

σ_{max} = maximum stress

σ_{min} = minimum stress

σ_{o1} = offset yield strength, 0.1%

σ_{uts} = ultimate tensile strength

1. Introduction

The implicit gradient method proved to be a powerful tool regarding the study of the fatigue life of welded structures in order to predict fatigue life for high- and medium-cycle fatigue for many different types of joints. The effective stress was calculated by following the same procedure and the same characteristic length was evaluated for thick welded joints [1–5]. In these papers, for the sake of simplicity, the welded joints were considered as a sharp V-notched component made of a linear elastic material. Therefore, regardless of the shape of the welded joint and its thickness, a unique fatigue scatter band was defined mainly because, in terms of nominal stress, the slopes of the Woehler curves were very close to each other [6]. Using this method, hundreds of experimental results were gathered into a single scatter band having a slope equal to 3 and intercept at $2 \cdot 10^6$ cycles equal to 151 MPa at 50% of life probability. The stress of 151 MPa was calculated by considering the effective principal stress mainly related to fatigue damage.

In the case of notched components, the classical theory, reported in many engineering design books, such as Collins [7], Jovinal and Marshek [8], Shigley [9] and Dowling [10], is able to predict the slope of the Woehler curve. The methodology is based on the work of Peterson [11] and Neuber [12] and keeps the strength of material fixed at low-cycle fatigue, so that, by changing the strength characteristics of the material at high-cycle fatigue, the Woehler curve moves and can fit the experimental data. However, these methods cannot be generalised to all components since this requires the definition of the stress concentration factor K_t that can be correlated to the fatigue strength reduction factor K_f. In order to overcome this problem, the scientific literature provides different methodologies based on an elasto-plastic local approach [13]. The effect of the non-linear behaviour of the material on K_f factors was taken into account, for example, by Ye and Wang [14]. The approach regards an energy point of view and K_f was calculated simply by using the plastic stain range $\Delta\varepsilon_p$ and the elastic strain range $\Delta\varepsilon_e$ acting on the cyclic.

The plastic $\Delta\varepsilon_p$ and elastic strain range $\Delta\varepsilon_e$ were obtained by means of the modified Neuber's relation [12–13].

One method that is widely adopted in the literature is the Smith Watson Topper (SWT) approach [15]. This method proposes a relation between the local value of maximum stress times the strain amplitude and the fatigue limits of parent materials. In this way, mean stress, the non-linear behaviour of the material and the notch effect are considered.

For threaded connections, the SWT approach was considered in reference [16] in conjunction with a simple model to describe the local cyclic creep as a function of stress amplitude. In order to improve the accuracy of the SWT method for Incoloy 901 superalloy and ASTM A723 steel, Ince and Glinka [17], proposed a modification of the SWT parameter. Recently, Kujawski [18] presented a new energy based interpretation of the SWT. In this case, the complementary strain energy densities were considered as the main cause of fatigue damage and then a deviatoric version of the SWT parameter was proposed. Both modifications of the SWT method appear promising, but as underlined by the authors themselves, the procedures should be re-examined using more experimental non-zero mean stress data sets in the future. Alternatively, as suggested by Dowling [19–20], the effect of the average stress of the cyclic hysteresis loop can be taken into account using Walker's model [21]. For smooth specimens, Dowling showed the efficacy of Walker's model for different materials and different levels of mean stress; material such as steel, aluminium alloy and titanium. By means of a new power exponent γ, Walker modified the classical Morrow fatigue life equations and introduced the nominal stress ratio R.

The SWT method is usually applied to stress at the notch tip but, as underlined in reference [22] and successively in reference [23], it could be extended to its average values. On the other hand, the designer can take into account not only the maximum local concentration factor but also a volume-averaged value as proposed by Neuber [12] (for a discussion on the characteristic lengths used in notch fracture mechanics, see reference [24] where four kinds of characteristic length parameters

were compared). Starting from the theory developed by Pluvinage in reference [25], other models based on non-linear material behaviour proposed the strain energy as a critical component n a critical volume near the notch [26–27]. The method assumes that the mean strain energy range, in the process volume where the damage takes place, has to be high enough in order to produce failure. The size of the process zone is situated in the high stressed region where the stress gradient is not too high. In this way, the effective distance that can be approximated with the diameter of a cylinder depends on the load level. Therefore, the effective distance is not considered as a material property as indeed it is considered in many others approaches [22, 28–32]. Another approach that changes the critical distance as a function of the load level was proposed in reference [33]. On the basis of the theory of the critical distance lifetime of notched components in the medium-cycle fatigue regime was estimated by considering an L distance between two extreme values (the characteristic length at high-cycle fatigue and the length for static problems) so far the L distance will be a function of the number of cycles to failure, N_f.

The aim of this paper is to extend the validity of the implicit gradient method procedure also for three-dimensional notched components made of ductile material at low- and medium-cycle fatigue life. A new non-linear procedure based on classical low cycled fatigue concept was proposed. In this way, a unique Woehler curve depending exclusively on the non-linear material proprieties can be defined based on Walker's model and by taking into account a constant material parameter independently of the load level. First of all, new experimental data relating to axisymmetric notched specimens, loaded with nominal stress ratio R=-1 and R=0, were presented. Then, the fatigue strength was assessed by means of the implicit gradient. Both the non-linear material (through FE) and the mean principal stress effect (through Walker) were considered. Finally, two-dimensional specimens made of FeP04 drawing steel and weakened by sharp lateral U and V-notches were investigated.

2. Experimental analysis

2.1 Specimen geometry

The tested specimens were taken from the extruded tube with an external diameter of 20 mm and a 5 mm diameter hole along the extrusion direction. Three different specimen geometries were machined through the turning process. Figure 1 shows the dimensions of the specimens and the geometry shape: smooth specimens (Fig. 1a); V-notched specimen (Fig. 2a) and semi-circular notched specimen (Fig. 1c).

Table 1 gives the values of stress concentration K_t, evaluated in relation to the nominal net section. K_t has been evaluated by means of a three-dimensional FE analysis under the hypothesis of linear elastic material behaviour. The values of K_t reported in Table 1 were obtained after a convergence analysis.

2.2 Chemical composition

This work was conducted using extruded low-carbon steel with 0.1% in weight of carbon. The material composition is shown in Table 2.

2.3 Microstructure analysis

Microstructure analysis was carried out using optical microscopy. The sample surface was polished with abrasive grinding paper up to 1200 grade and subsequently the final finishing was carried out with 1 µm suspension solution. Therefore, the etching of the underlined surface using NITAL4

reagent allowed for grain visualisation. Figure 2 shows the microstructure along the axial direction (extrusion direction) and the radial direction.

The black areas in the figure depict pearlite and the white areas depict ferrite. Small spots within the ferrite grains are inclusions or impurities such as oxides and sulphides. The grains of ferrite have an average size of about 25 µm and the pearlite grains were slightly smaller.

The hardness test was conducted on parent material before the turning machining. As it is possible to see from Vickers' profile (Fig. 3), the external zone, around the perimeter, presented minor values of hardness along a radial extension of about 1.5 mm. This phenomenon can be attributed to surface decarburisation taking place after extrusion. In fact, the decarburised surface did not show the pearlite. Machinability is poor in this region. Fortunately, the volume where the decarburisation took place was removed by turning to obtain the desired diameter size. However, an average value of 181 HV was obtained. The ultimate tensile strength estimated through Vickers' Hardness is consistent with that found with the tensile test and is shown later.

2.4 Static proprieties

Tensile and fatigue tests were carried out at room temperature by means of an MTS hydraulic testing machine with a force range of ±250 kN. Table 3 reports the monotonic material proprieties such as elastic modulus E, the ultimate tensile strength σ_{uts}, the strength hardening coefficient k and the strain hardening exponent n according to the Ramberg-Osgood equation:

$$\epsilon = \frac{\sigma}{E} + \left(\frac{\sigma}{k}\right)^{\frac{1}{n}} \quad (1)$$

A plot of the monotonic stress-strain curve is reported in Figure 4. Reference strength $R_{p01\%}$ may be defined which corresponds to a 0.1% plastic strain offset on the monotonic curves.

2.5 Fatigue test results

The axial symmetric specimens were tested under fatigue sinusoidal axial loading at constant stress or stain amplitude. The applied load frequency was modulated as a function of the load magnitude in order to prevent the specimen from overheating and subsequent undesirable effects; the frequency range was from 1 Hz to 20 Hz.

The fatigue tests, on smooth specimens, were performed both in stress control (for high-cycle fatigue) and in strain control (for low-cycle fatigue). Strain was measured using a 10 mm gauge length extensometer over the 16 mm straight part of the smooth specimen. From fatigue tests on smooth specimens, it was possible to procure the stabilised behaviour of the material and then the cyclic stress-strain curve (Fig. 4). A direct comparison with the monotonic stress-strain curve shows that the material is a strain softening steel. The Ramberg-Osgood relation can also be used for the mathematical representation:

$$\epsilon = \frac{\sigma}{E} + \left(\frac{\sigma}{k\prime}\right)^{\frac{1}{n\prime}} \tag{2}$$

The cyclic strength hardening coefficient *k'* and the cyclic strain-hardening exponent n' are reported in table 3. As in the case of monotonic loading, a reference stress $R'_{p01\%}$ may be defined that corresponds to a 0.1% plastic strain offset on the cyclic stress-strain curve.

The Manson-Coffin relationship is generally used to describe the strain-life curves mathematically:

$$\varepsilon_a = \frac{\sigma_f^{'}}{E}\left(2\,N_f\right)^{b^{'}} + \varepsilon_f^{'}\left(2\,N_f\right)^{c^{'}} \tag{3}$$

where N_f is the cycle to failure. However, Eq. (3) does not take into account the effect of the mean stress of the stabilised hysteresis loop.

As widely discussed by Dowing in refs [19–20], Walker's model [21] is able to consider the effect of mean stress by using a further exponent γ. Dowling summarised Walker's model in the form [19]:

$$\varepsilon_a = \frac{\sigma_f{}'}{E}\left(\frac{1-R}{2}\right)^{(1-\gamma)}(2N_f)^b + \varepsilon_f{}'\left(\frac{1-R}{2}\right)^{\frac{c(1-\gamma)}{b}}(2N_f)^c \qquad (4)$$

R being the stress ratio of the stabilised-strain hysteresis loop. The model is defined for smooth specimens i.e. for a uniform stress and strain field along the straight region. Dowling showed that Walker's model works well for a high number of strain-life data sets with non-zero mean stress, such as steel and aluminium alloys. In order to find a single fit-curve between the strain amplitude and a cyclic life parameter, in ref. [20], Dowling considers the equivalent life N_{fw} from Walker's model as:

$$N_{fw} = N_f\left(\frac{1-R}{2}\right)^{\frac{(1-\gamma)}{bw}} \qquad (5)$$

Eq. (2) by means of Eq. (3) can be rewritten in the form:

$$\varepsilon_a = \frac{\sigma_f{}'}{E}(2\cdot N_{fw})^{bw} + \varepsilon_f{}'(2\cdot N_{fw})^{cw} \qquad (6)$$

when R=-1 Walker's equivalent cycles N_{fw} agrees with the cycle to failure.

In reference [19], about twenty data sets of smooth specimens made of dissimilar materials and characterised by different levels of mean stress, fit the experimental data by using a single fitting curve (6). Walker's parameter γgives a versatility that the other common mean stress methods do not have.

The fatigue life curve (6) requires five parameters to be defined. The best fitting of the experimental data of the smooth specimens has been proposed since Walker's report (6) provides an

opportunity to fit fatigue life data all together at various mean stresses. These five parameters are obtainable through a fitting process that includes at least two different load ratio R sets of experimental data. The values obtained in the best-fitting analysis are reported in table 4, whereas Figure 5 shows the experimental data of smooth specimens under remote tensile loading with R equal to -1 and 0, respectively.

Concerning the fatigue life of notched specimens, Figure 6 and 7 reports the Woehler curves where the amplitude of nominal stress gives fatigue life between 10^4 and $3 \cdot 10^6$ cycles. The fatigue limit, evaluated at $2 \cdot 10^6$ cycles, is reported in these figures.

Typical failure sections obtained during the experimental phase are reported in Figure 8

3. The use of the implicit gradient approach

The geometrical effect on fatigue can be studied by introducing an equivalent or effective stress that is evaluated inside a region near the notch tip where a fatigue crack usually occurs. In their well-known papers, Neuber and Peterson [11–12] propose to consider an average value of a stress or strain value, at a characteristic distance from the notch tip. Some years later, Sheppard [28] extended the idea to a semi-circular area at the notch tip considering the average of the maximum principal stress. In ref. [29], Taylor resumes the methods relating to a critical distance that depends on material proprieties and shows its potentiality to calculate the fatigue limits for notches and cracks by means of a critical distance approach.

From a theoretical point of view, the implicit gradient approach generalises the idea of effective stress relating to an average value of a physical parameter. In fact, it was demonstrated in [2] that all the critical distance approaches can be obtained by means of a specific value of a weight function that

controls the value of the physical parameter inside the whole component and not only inside a limited region at the vicinity of the notch tip.

According to the non-local theory proposed by G. Pijaudier-Cabot and Z.P. Bažant [34–35], an effective scalar ζ_{eff}, in the generic point P of the domain, can be defined from the average of its local counterpart, ζ_{eq}, weighted by function α:

$$\zeta_{eff}(P) = \frac{\int_V \alpha(P,Q)\, \zeta_{eq}(Q)\, dV}{\int_V \alpha(P,Q)\, dV} \tag{7}$$

where Q is a point inside volume V and the equivalent scalar ζ_{eq} is a function of the stress tensor. The weight function α is an isotropic function of the distance $|PQ|$, which vanishes as distance $|PQ|$ increases.

To overcome the evaluation of the integral (7) overall volume V for each point **P** of V, Peerlings et al. [36] proposed an alternative calculation. After a Taylor expansion of Eq. (7), the evaluation of effective scalar $\zeta_{eff,}$ when α is a proper isotropic function, can be substituted by the solution of a differential equation in volume V (for more details, see refs [36] and [37]):

$$\zeta_{eff} - \bar{c}^2 \nabla^2 \zeta_{eff} = \zeta_{eq} \qquad in \quad V \tag{8}$$

where $\bar{c}$ is a characteristic length related to the weight function $\alpha(P,Q)$ defined on the whole volume V and ∇^2 denotes the Laplacian operator. As assumed in previous papers [37], we consider that $\bar{c}$ depends only on the material. Other more complicated choices are possible [38] but they are not dealt with here.

Note that Eq. (6) can also be obtained by applying the strain gradient elasticity theory developed by Aifantis in many papers (see, for example, ref. [39]).

In this paper, to solve the inhomogeneous Helmholtz equation (8), we consider a Neumann-type boundary condition:

$$\nabla \zeta_{eff} \cdot n = 0 \qquad \text{on} \quad \partial V \tag{9}$$

where **n** is the outward normal to the boundary and the symbol ∇ indicates the gradient operator.

Under a monoaxial fatigue loading, the variations of the effective scalar are directly considered. Indeed, under multiaxial fatigue, the procedure is more complex and further elaboration is needed [3, 40].

In previous papers we considered a material with linear elastic behaviour. In these cases only two FE numerical analyses were necessary. The first analysis was used for evaluate the standard Cauchy stress tensor, the second analysis was necessary for solve the Helmholtz differential equation (8) by means of a PDE solver. In order to optimize the procedure we can use the same mesh for both FE analysis.

The efficiency of the implicit gradient approach for sharp notches has been shown in different papers [1–5]. By solving the differential equation (8) in the volume V, the designer evaluates the effective scalar parameter ζ_{eff} at each point of the mechanical component with a single post-processing FE numerical analysis. On the contrary, by means of equation Eq. (7), the integral must be iterate in the entire volume for each node of the FE model. On the other hand, if the designer is only interested in knowing the stress at the notch tip, a simplified procedure is suggested in ref. [41].

In the previous paper, by taking into account welded joints made of steel with a linear elastic behaviour [1], the choice of first principal stress as effective equivalent ζ_{eq} gave good results in the range of 10^4 to $5 \cdot 10^6$ cycle fatigue. The equivalent scalar parameter ζ_{eff}, as well as the value of $\bar{c}$, for steel welded structures was always the same independently of the weld shape or the thickness of the main plate.

For rounded notches [42], indeed, the gradient approach was considered only at high-cycle fatigue because the choice of a linear elastic material behaviour was no longer able to move the slope of the Woehler curve. In these cases the value of $\bar{c}$ was different from each series of experimental set as a function of El-Haddad's critical length [43].

4. Non-linear implicit gradient approach for finite fatigue life: a new procedure

In order to evaluate the fatigue life in the whole range of a number of cycles, starting from the low-cycle fatigue, the schematisation of the linear elastic material is no longer applicable. Due to the dependence between the notch severity and the correspondent Wohler curve slope, an alternative approach is needed. The idea is to take into account the non-linear material behaviour in the FE model in order to adjust the slopes of the fatigue life curve and resume the experimental points in relation to different geometry in a unique, relatively narrow, scatter band in the Woehler diagram. The procedure is subdivided into three steps. First of all, two non-linear FE analysis is performed namely *A-FE* and *B-FE*. In analysis *A-FE* the load is the maximum load and the σ–ε curve is the stabilised curves. In analysis *B-FE* the load is the range of the applied load and the σ–ε curve is the double of the stabilised curves (Massing behaviour, see Figure 9).

The second step of the procedure solves the Helmholtz differential equation (6) and evaluates the effective parameter by using the same mesh previously defined in the non-linear FE analysis and the desired component of the strain or stress tensor as input. Therefore, three new equivalent parameters are evaluated: the maximum equivalent stress $\sigma_{max,eff}$ from *A-FE analysis* results, the range of the effective strain $\Delta\varepsilon_{eff}$ from *B-FE analysis* results and the range of the effective stress $\Delta\sigma_{eff,}$ from *B-FE analysis*. These new parameters assume the same nomenclature of the primary physical parameter but add the subscript *eff*. $\sigma_{eff,max}$ is calculated by imposing ζ_{eq} in equation (8) equal to the principal stress obtained from *A-FE* analysis, $\Delta\varepsilon_{eff}$ is calculated by imposing ζ_{eq} equal to the principal strain

obtained from *B-FE analysis*, $\Delta\sigma_{eff}$ is calculated by imposing ζ_{eq} equal to the principal stress obtained from *B-FE analysis*.

The third step evaluates the fatigue life of the component. By defining

$$\varepsilon_{a,eff} = \frac{\Delta\varepsilon_{a,eff}}{2} \tag{10}$$

$$\sigma_{mean,eff} = \frac{\Delta\sigma_{eff}}{2} \tag{11}$$

$$R_{\sigma,eff} = \frac{\sigma_{min,eff}}{\sigma_{max,eff}} \tag{12}$$

it is possible to use strain-life equation (6) via the effective parameters at the notch tip:

$$\varepsilon_{a,eff} = \frac{\sigma_f{}'}{E}(2 \cdot N_{fw})^{bw} + \varepsilon_f{}'(2 \cdot N_{fw})^{cw} \tag{13}$$

$$N_{fw} = N_f \left(\frac{1-R_{\sigma,eff}}{2}\right)^{\frac{(1-\gamma)}{b}} \tag{14}$$

In this way, it is possible to obtain a single fatigue scatter band depending exclusively on the material and defined only from smooth specimen materials proprieties. Independently of notch severity, Figure 9 resumes the material proprieties used in the analysis.

In order to solve Eq. (8), the value of $\bar{c}$ is needed. For welded joints made of steel, this value was proved to be 0.2 mm [1–3]. In general, if a linear elastic behaviour of the material is recognised, $\bar{c}$ could be calculated from the following relationship:

$$\bar{c} = z\ a_0 \tag{15}$$

where z depends on the choice of the equivalent stress (for ζ_{eq} equal to the maximum principal stress, z becomes 0.545 [37]) and a_0 is El-Haddad's critical length [43] defined by the fatigue limit of the parent material and the ΔK_{th} threshold range of the Stress Intensity Factor.

$$a_0 = \frac{1}{\pi}\left(\frac{\Delta K_{th}}{\Delta \sigma_0}\right)^2 \tag{16}$$

Due to the non-linear behaviour of the material, an alternative way is considered in this paper. From experimental analysis with R=-1, the value of fatigue limits at $2 \cdot 10^6$ cycles of sharp V-notch is known, so with a non-linear analysis the value of $\bar{c}$ can be found by imposing that the effective parameter will be equal to the corresponding value of the smooth specimen. The analysis of the low carbon steel alloy presented in section 3, shows that we can use a value of $\bar{c}$ equal to 0.12 mm for strain effective analysis and it was considered the same for the three numerical analyses of Eq. (8). The value of $\bar{c}$ can be obtained from a figure that plots the effective values ζ_{eff} of a sharp notch versus $\bar{c}$ such as in Figure 10. The effective values ζ_{eff} for the low alloy steel used in the experimental analysis was obtained from the experimental data of V-notched specimens under the load case *R=-1*. The horizontal line represents the effective parameter evaluated on smooth specimens at $2 \cdot 10^6$ cycle fatigue.

5. Comparison with experimental data.

5.1 Axisymmetric specimens

The SWT parameter can be used for the evaluation of the fatigue life under a non-zero mean stress including non-linear analysis.

$$\epsilon_a \sigma_{max} = f\left(2\, N_f\right) \tag{17}$$

Where $f(2{\cdot}N_f)$ is the Manson-Coffin fatigue-life curve of smooth specimen. Figure 11 shows the SWT parameter calculated with FE analysis at the notch tip for all the experimental data presented in Figures 6 and 7. The SWT parameter differs from the parent material behaviour; however, the method underestimates the fatigue life of notched components (Fig. 10).

At this point, the fatigue life estimation has been conducted using Walker's equation (6) where the effective loading ratio and the effective strain amplitude stress were calculated with implicit gradient equation (8). Since the aim of this work is to define a general procedure for fatigue life assessments, the effective strain amplitude of all the experimental data against Walker's fatigue life parameter $N_{f,w}$ was considered in Figure 12. The scatter is drastically reduced with respect to Figure 11.

5.2 Plane specimen with lateral U and V-notches

The proposed method, based on a non-linear gradient approach, is used for evaluating the fatigue proprieties of specimens reported in Figure 13. The experimental analysis has been carried out in reference [22]. In this paper, we consider the results relative to FeP04 deep drawing steel without distinguishing between the initiation and propagation phase. For the sake of simplicity, the specimen characterised with an opening angle $2\alpha=70°$, was considered as a full V-notch despite a U-notch with a final sharp V-notch. Table 5 reports the geometrical proprieties of specimens considered in the analysis. The value of $\bar{c}$ obtained with the non-linear procedure was 0.47 mm.

Figure 14 shows the results in terms of the nominal stress referred to in the net section. The scatter between the experimental data drastically decreases as soon as we consider the proposed non-linear analysis. Figure 15 reports the effective strain amplitude versus Walker's life parameter for all sample data sets analysed.

6. Conclusions

The evaluation of fatigue life at low- and medium-cycle fatigue for notched components has been obtained by means of the implicit gradient approach. According to the physical parameter defined in the classic low-cycle fatigue procedure the definition of effective quantities overcame the problem of a notched component made of ductile material. The method is particularly suitable for three-dimensional analysis as well as for two-dimensional analysis without introducing geometric exemplifications. The characteristic length of the material is considered constant and was evaluated by means of a non-linear procedure.

The use of Walker's model has allowed us to evaluate the influence of the average stress on fatigue life as a function of local plasticisation, more or less extensive, due to the variation of the applied load. Furthermore, a unique Woehler curve is defined as a function of Walker's equivalent life valid for all notched components.

Acknowledgement

The authors wish to thank the Italian Ministry of University and Scientific Research for funding this research under Grant PRIN 009Z55NWC_002.

References

[1] R. Tovo, P. Livieri. An implicit gradient application to fatigue of sharp notches and weldments. Engineering Fracture Mechanics, 74, 2007, 515–526

[2] R. Tovo, P. Livieri, A numerical approach to fatigue assessment of spot weld joints. Fatigue and Fracture of Engineering Materials and Structures, Volume 34, Issue 1, 2011, Pages 32–45

[3] A. Cristofori, P. Livieri, R. Tovo, An Application of the Implicit Gradient Method to welded structures under multiaxial fatigue loadings. International Journal of Fatigue, Volume 31, Issue 1, Pages 12–19, 2009

[4] P. Livieri, R. Tovo, The effect of throat underflushing on the fatigue strength of fillet weldments, Fatigue & Fracture of Engineering Materials & Structures, Volume: 36 Issue: 9 Pages 884–892

[5] R. Tovo, P. Livieri, A numerical approach to fatigue assessment of spot weld joints. Fatigue and Fracture of Engineering Materials and Structures, Volume 34, Issue 1, 2011, Pages 32–45

[6] D. Radaj, C.M. Sonsino, W. Fricke, Fatigue assessment of welded joints by local, approaches. 2nd ed. Cambridge: Woodhead Publishing and Boca Raton Fla: CRC Press; 2006

[7] J. A. Collins, Failure of Materials in Mechanical Design*:* Analysis*, Prediction, Prevention, 2nd ed., Wiley, New York, 1993*

[8] R.C. Juvinall, K. M. Marshek, Mechanical Engineering Design, 5th ed., McGraw-Hill, New York

[9] J.E. Shigley, Mechanical Engineering Design, Ninth Edition, R. G. Budynas J. K. Nisbett, McGraw-Hill, 2011

[10] N. E. Dowling, *Mechanical Behavior of Materials*, Prentice–Hall, 1993

[11] Peterson RE. Notch-sensitivity. In: Sines G, Waisman JL, editors. Metal fatigue. New York: McGraw Hill; 1959

[12] H. Neuber, Uber die Berucksichtigung der Spannungskonzentration bei Festigkeitsberechnungen. Konstruktion 1968; 20 (7): 245–51

[13] T.H.Topper, R.M.Wetzel, J. Morrow. *Neuber's Rule Applied to Fatigue of Notched Specimens*, Journal of Materials, JMLSA, Vol.4, No.1, March 1969, Pages 200–209

[14] D.-Y. Ye, D.-J. Wang – A new approach to the prediction of fatigue notch factor K_f, International Journal of Fatigue Vol.18 no.2 Pages 105–109, 1996

[15] K.N. Smith, P. Watson, and T.H. Topper, A stress-strain function for the fatigue of metals. *Journal of Materials, JMLSA,* 1970, 5, 767–778

[16] R. Schnreider, U. Wuttke, C Berger, Fatigue analysis of threaded connections using the local strain approach, Procedia Engineering, 2, 2010, 2357–2366

[17] Ince, G. Glinka – *A modification of Morrow and Smith-Watson-Topper mean stress correction models*, Fatigue & Fracture of Engineering Materials & Structures 34, 854–867, 2011

[18] Daniel Kujawski, A deviatoric version of the SWT parameter, International Journal of Fatigue, *Volume 67*, *October 2014*, *Pages 95–102*

[19] N.E. Dowling – *Mean stress effect in strain-life fatigue*, Fatigue & Fracture of Engineering Materials & Structures 32, 1004–1019, 2009

[20] N.E. Dowling, C.A. Calhoun, A. Arcari, *Mean stress effects in stress-life fatigue and the Walker Equation*, Fatigue & Fracture of Engineering Materials & Structures 32, 163–179, 2009

[21] K. Walker, (1970) The effect of stress ratio during crack propagation and fatigue for 2024-T3 and 7075-T6 aluminum. *Effects of Environment and Complex Load History on Fatigue Life*. ASTM STP 462, Am. Soc. for Testing and Materials, Philadelphia, PA, Pages 1–14.

[22] P. Lazzarin, R. Tovo, G. Meneghetti, (1997) Fatigue crack initiation and propagation phases near notches in metals with low notch sensitivity. *International Journal of Fatigue* **19**, 647–665

[23] L. Susmel, D. Taylor, An Elasto-Plastic Reformulation of the Theory of Critical Distances to Estimate Lifetime of Notched Components Failing in the Low/Medium-Cycle Fatigue Regime, ASME, Journal of Engineering Material and Technology, 2010, Vol. 132

[24] G. Pluvinage. J. Capelle, On characteristic lengths used in notch fracture mechanics, Int J Fract (2014) 187:187–197

[25] G. Pluvinage, Notch effect in high cycle fatigue. ICF9 Sydney, 1997

[26] G. Qylafku, Z. Azari, N. Kadi, M. Gjonaj, G. Pluvinage. Application of a new model proposal for fatigue life prediction on notches and key-seats, *International Journal of Fatigue*, *Volume 21, Issue 8*, *September 1999*, *Pages 753–760*

[27] S. Bentachfine, G. Pluvinage, J. Gilgert, Z. Azari, D. Bouami, Notch effect in low cycle fatigue*, International Journal of Fatigue*, *Volume 21, Issue 5*, *May 1999*, *Pages 421–430*

[28] S.D. Sheppard, Field effects in fatigue crack initiation: long life fatigue strength. Trans ASME 1991;113:188–194

[29] D. Taylor (1999) Geometrical effects in fatigue: a unifying theoretical model. *Int. J. Fatigue* 21, 413–420

[30] F. Berto , P. Lazzarin, Recent developments in brittle and quasi-brittle failure assessment of engineering materials by means of local approaches, Materials Science and Engineering R 75 (2014) 1–48

[31] P. Livieri, "A new path independent integral applied to notched components under mode I loadings ", International Journal of Fracture, October 2003, Volume 123, Issue 3-4, Pages 107–125

[32] P. Livieri, R. Tovo, The use of the J_V parameter in welded joints: stress analysis and fatigue assessment. International Journal of Fatigue, Volume 31, Issue 1, Pages 153–163, January 2009

[33] L. Susmel, D. Taylor, A novel formulation of the theory of critical distances to estimate lifetime of notched components in the medium-cycle fatigue regime, Fatigue Fract Engng Mater Struct 2007, 30, 567–581

[34] G. Pijaudier-Cabot and Z.P. Bažant, Nonlocal Damage Theory, Journal of Engineering Mechanics, 10 (1987) 1512–1533

[35] Z.P. Bažant, Imbrigate continuum and its variational derivation, Journal of the Engineering Mechanics Division, ASCE, 110, 12,1984, Pages 1693–1712

[36] R.H.J. Peerlings, R. de Borst, W.A.M. Brekelmans, J.H.P. de Vree, Gradient enhanced damage for quasi-brittle material. International Journal of Numerical Methods in Engineering 39, 1996, 3391–3403

[37] R. Tovo, P. Livieri, E. Benvenuti, An implicit gradient type of static failure criterion for mixed-mode loading. International Journal of Fracture 141, Pages 497–511, 2006

[38] M.G.D. Geers, R.H.J. Peerlings, R. de Borst, W.A.M. Brekelmans, "Validation and internal length scale determination for a gradient damage model: application to short glass-fibre-reinforced polypropylene". International Journal of Solids and Structures, **36**, 2557–2583, 1999

[39] E.C. Aifantis. Update on a class of gradient theories. Mechanics of Materials, **35**, 2003: 259–280

[40] S. Capetta, R. Tovo, D. Taylor, P. Livieri. Numerical evaluation of fatigue strength on mechanical notched components under multiaxial loadings, International Journal of Fatigue 33 (2011) 661–671

[41] E. Maggiolini, P. Livieri, R. Tovo, Implicit gradient and integral average effective stresses: relationships and numerical approximations, Fatigue & Fracture of Engineering Materials & Structures, in print

[42] R. Tovo, P. Livieri, An implicit gradient application to fatigue of complex structures, Engineering Fracture Mechanics, 75 (7), 2008, 1804–1814

[43] M. H. El Haddad, T.H. Topper, K. N. Smith, Fatigue crack propagation of short cracks. ASME, Journal of Engineering Material and Technology 101, 1979, 42–45

Table 1: Linear elastic stress concentration factors for axial loading (referred to net section)

Specimen	K_t
smooth	1.02
semi-circular	1.55
V-notched	5.79

Table 2: Chemical composition (percent values)

C	Si	Mn	P	S	Ni	Al	Cu	Ti	V
0.118	0.192	0.413	0.013	0.00202	0.026	0.0263	0.018	0.00196	0.00189

Table 3: Stress – strain curve parameters

E [MPa]	σ_{uts} [MPa]	$R_{p01\%}$ [MPa]	***K*** [MPa]	***n***	$R'_{p01\%}$ [MPa]	***K'*** [MPa]	***n'***
197000	552	408	820	0.14	552	502	0.0677

Table 4: Parameters for strain-life curve (4)

σ'_f [MPa]	ε'_f	b_w	c_w	γ
697	33.7	-0.078	-1.04	0.882

Table 5: Specimens made of FeP04 deep drawing steel [22]

Series	2α **[deg]**	ρ
R1.25	0	1.25
R2.5	0	2.5
R10	0	10
70°	70	0.2
90°	90	0.2

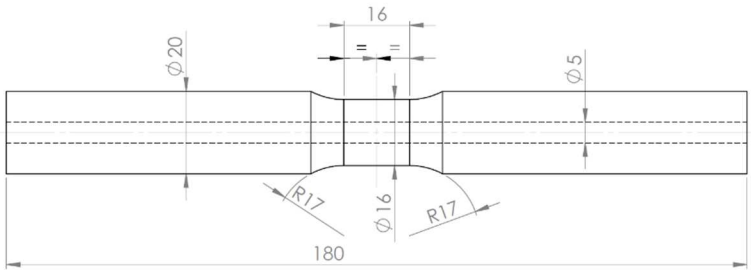

a

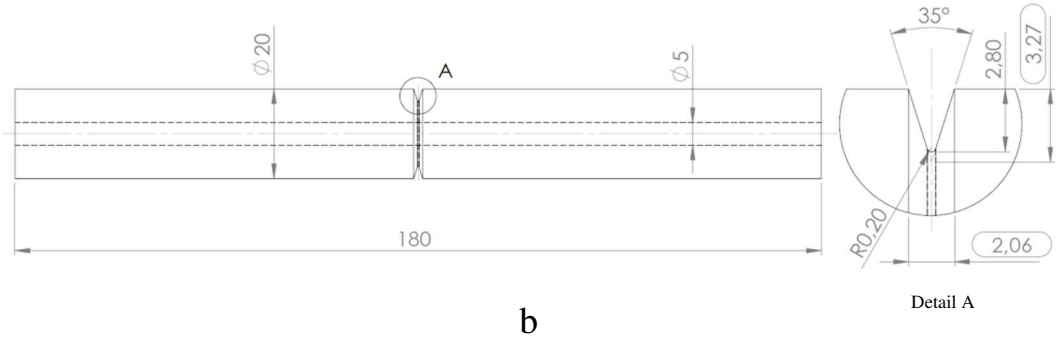

b

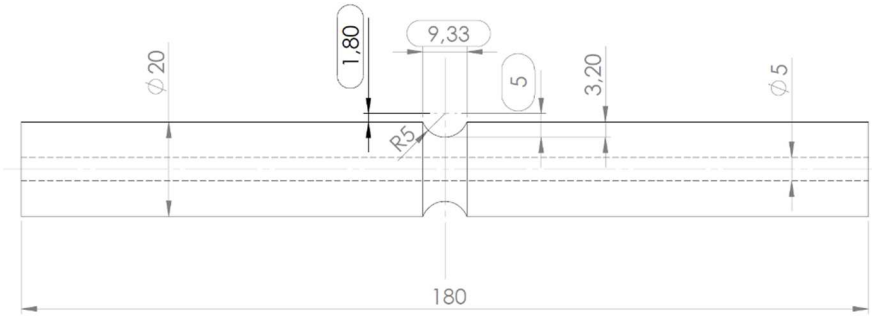

c

Figure 1: Axisymmetric specimen geometry: a) Smooth specimen; b) V-notched specimen; c) Semi-circular notched specimen (dimensions in millimetres)

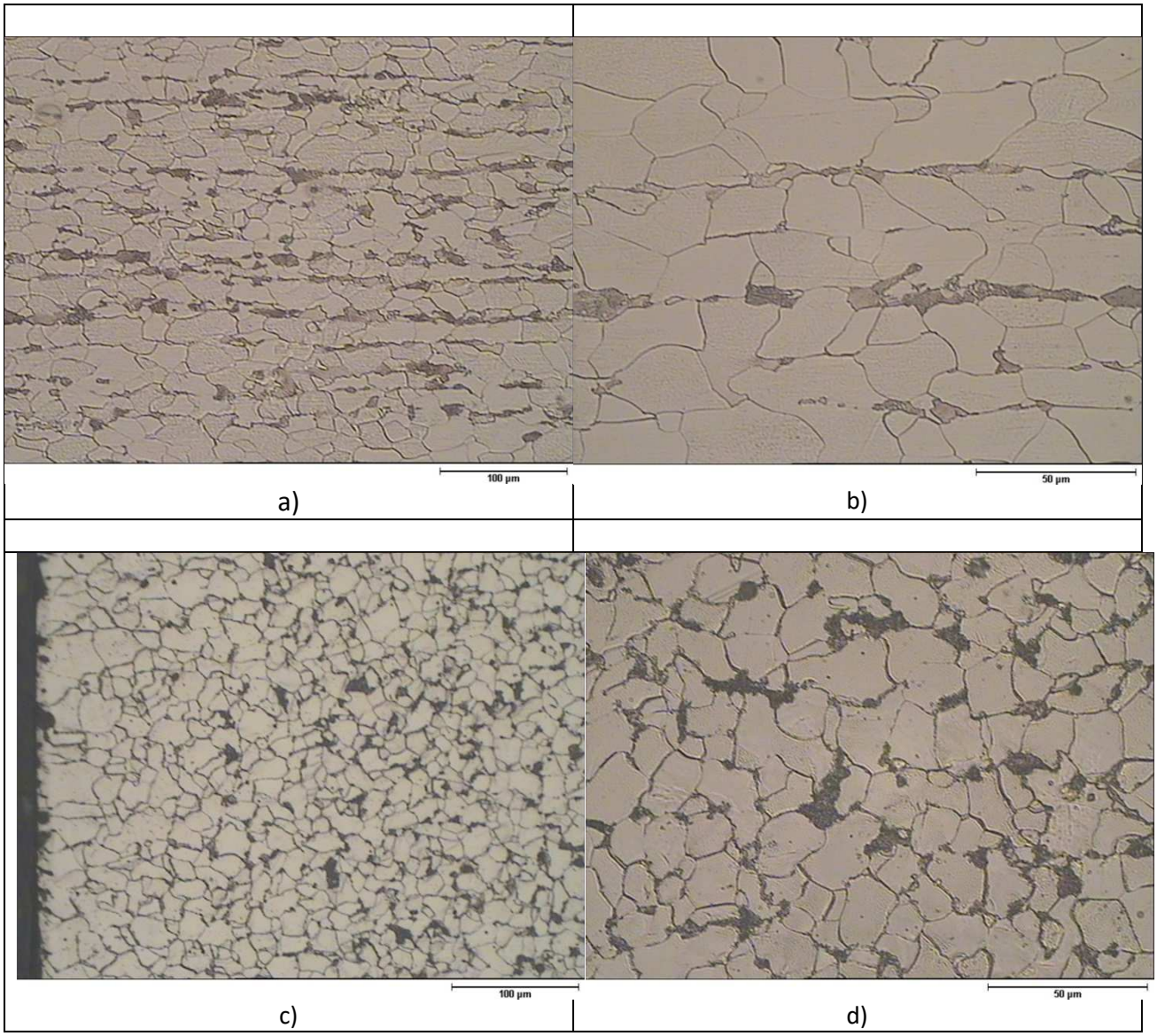

Figure 2: Microstructure specimen: *a* and *b* axial direction (extruding direction); *c* and *d* radial direction

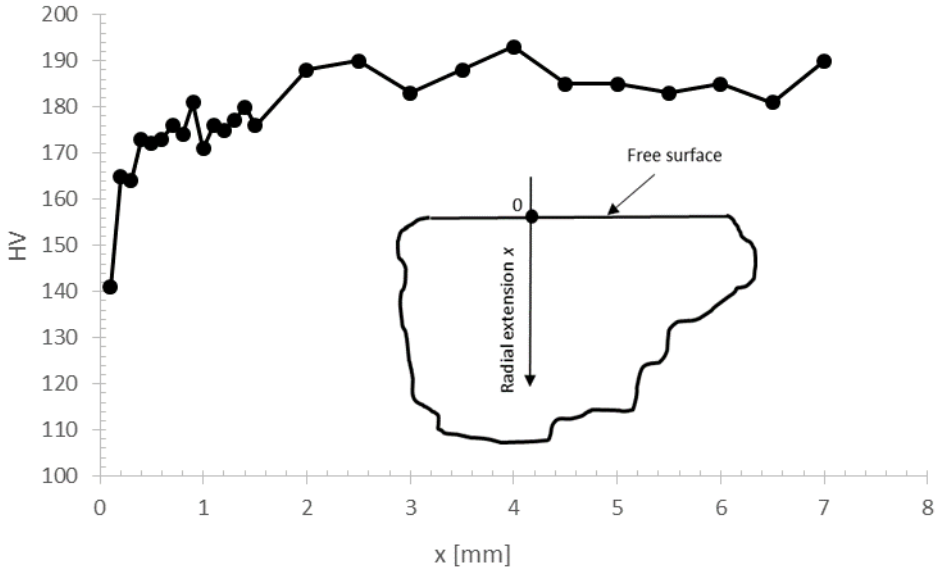

Figure 3: Vickers' profile along the radial direction (surface x=0)

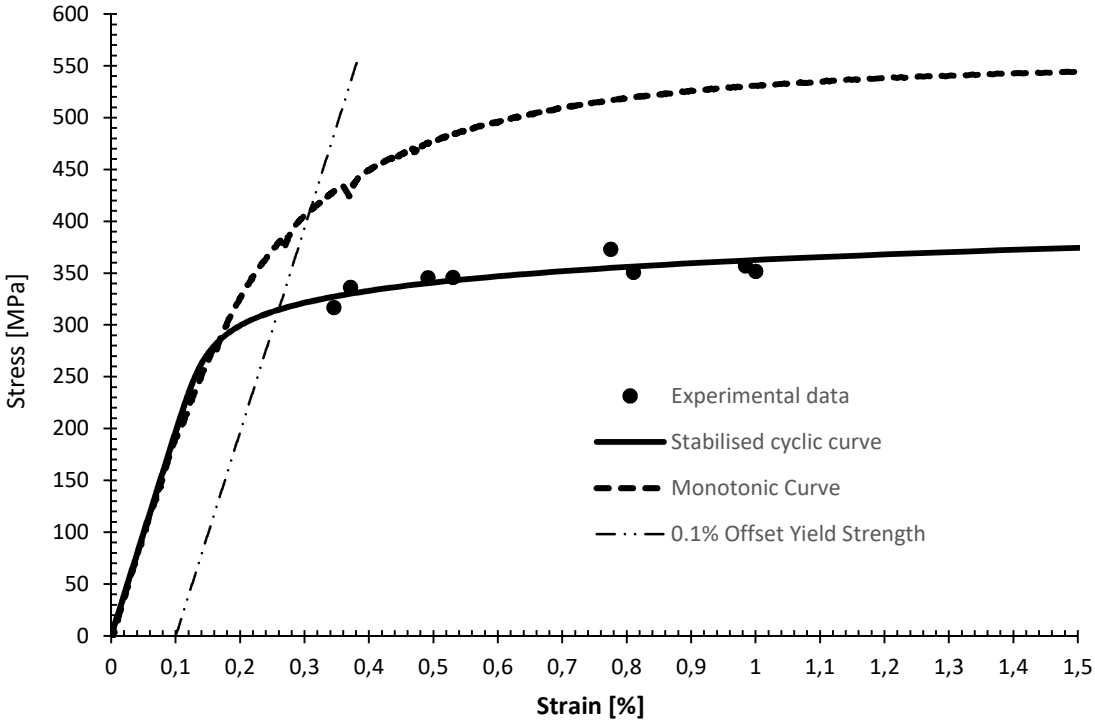

Figure 4: Monotonic and cyclic stress-strain curves

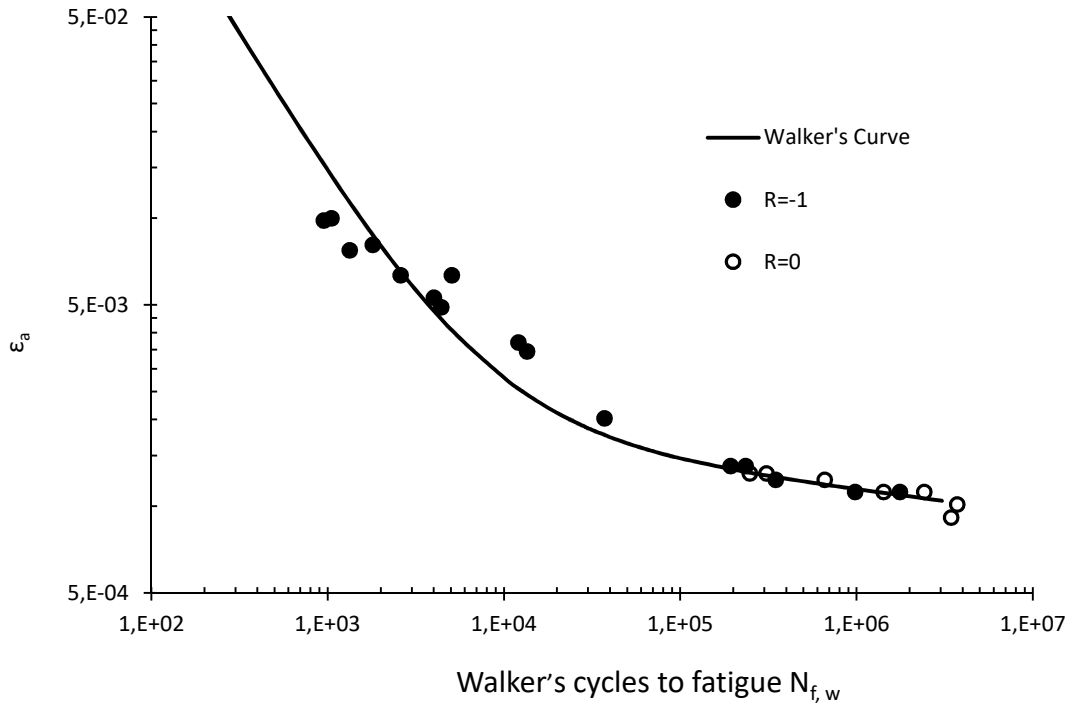

Figure 5: Experimental data of smooth axisymmetric specimens and Walker–equivalent-life curve

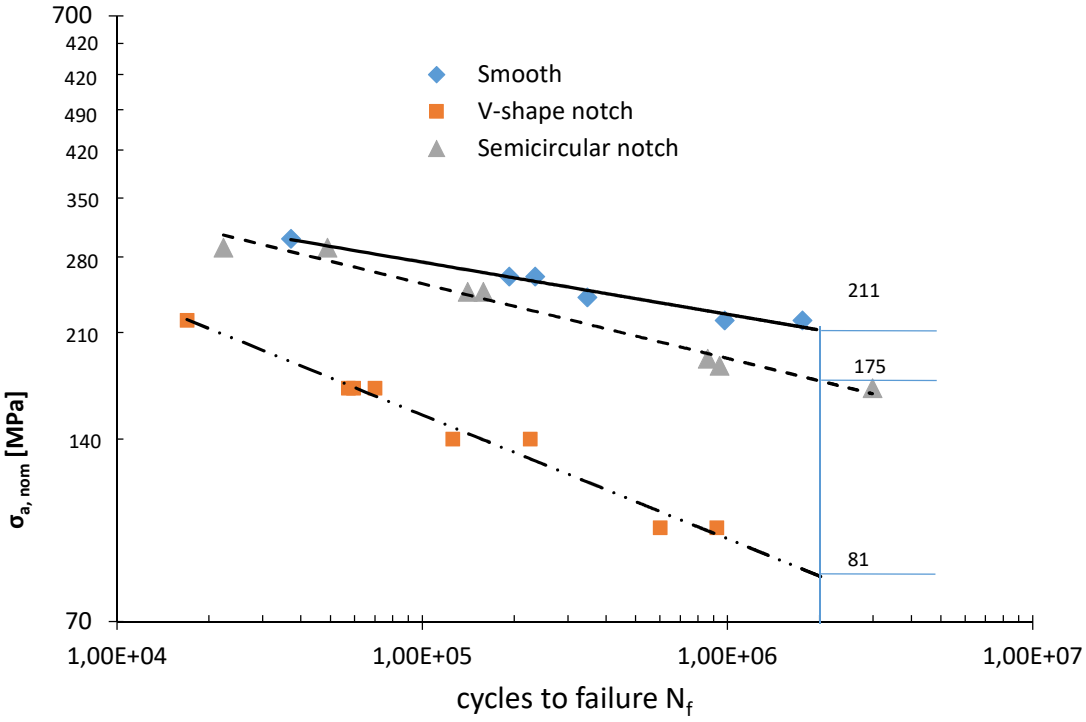

Figure 6: Fatigue life of axisymmetric specimens for nominal stress ratio R=-1

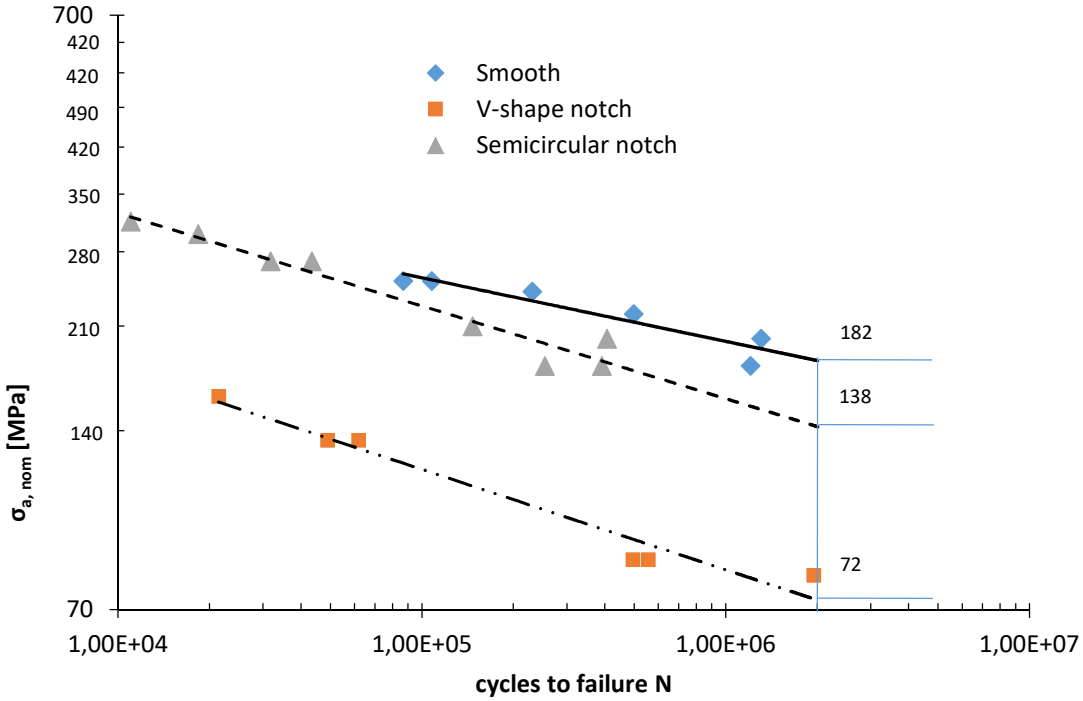

Figure 7: Fatigue life of axisymmetric specimens for nominal stress ratio R=0

The right reference [31]

Livieri P. Use of J–integral to predict static failures in sharp V-notches and rounded U-notches. Eng Fract Mech 2008;75:1779-93

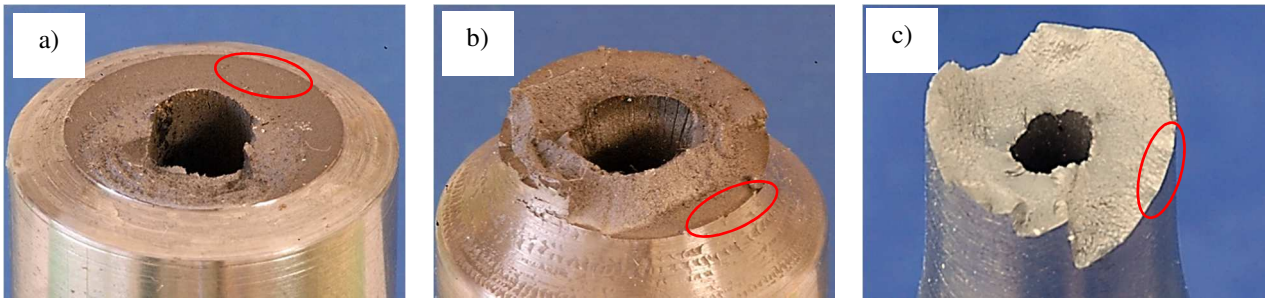

Figure 8: Fracture surfaces. Circled in red the crack nucleation site. a) V-notched specimen; b) semi-circular notch specimen; c) smooth specimen

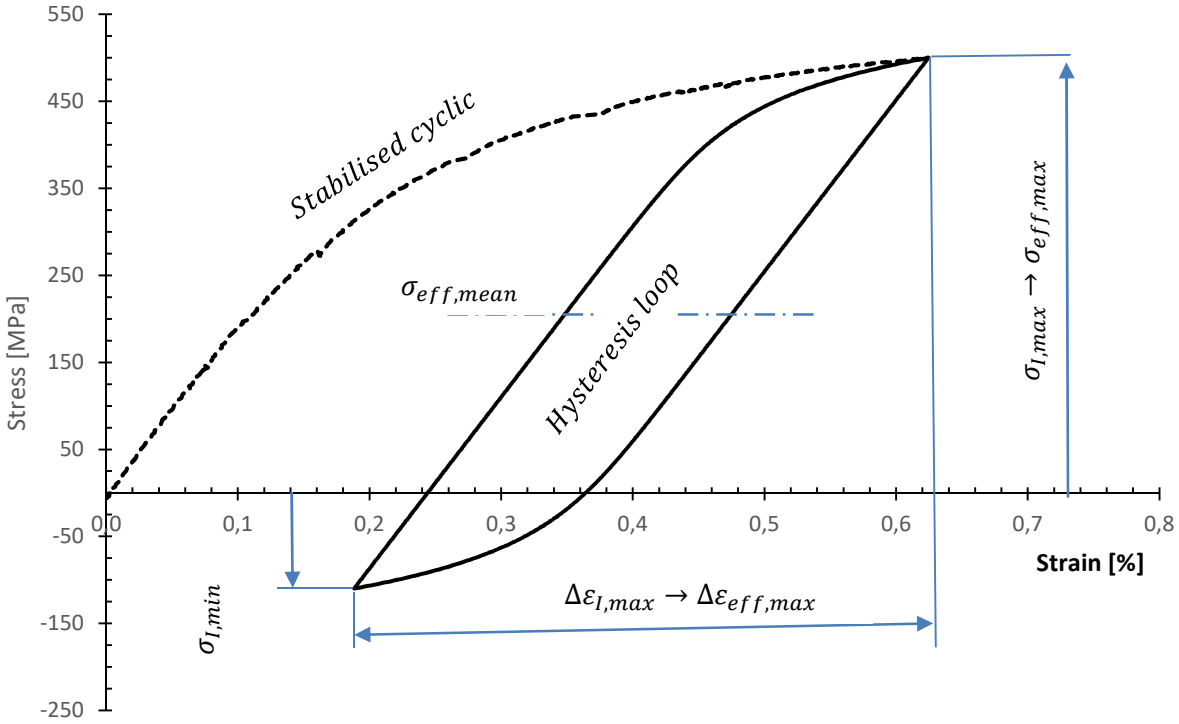

Figure 9: Stress and strain at the notch tip in the FE analysis

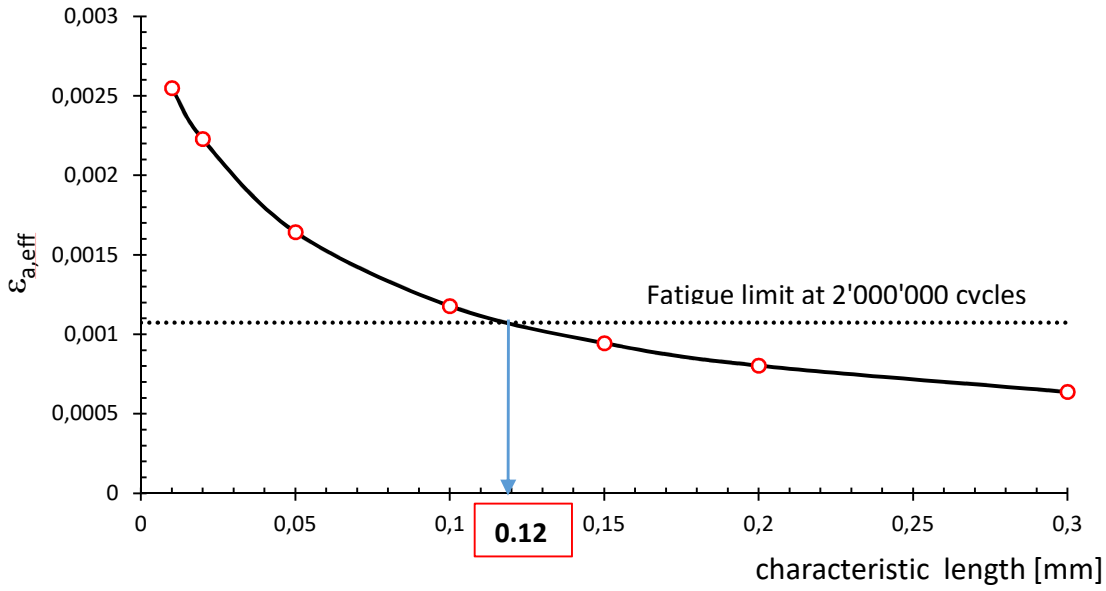

Figure 10: Value of $\bar{c}$ obtained at $2 \cdot 10^6$ cycle fatigue for axisymmetric specimens

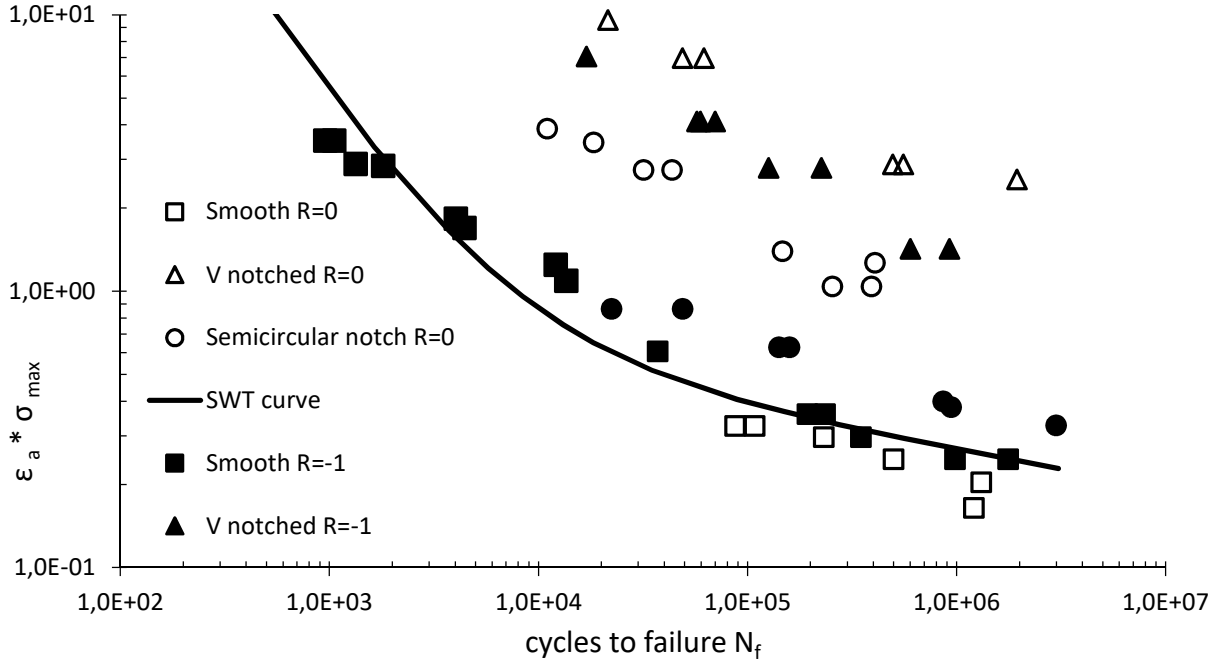

Figure 11: SWT parameter versus cycle fatigue for axisymmetric specimens

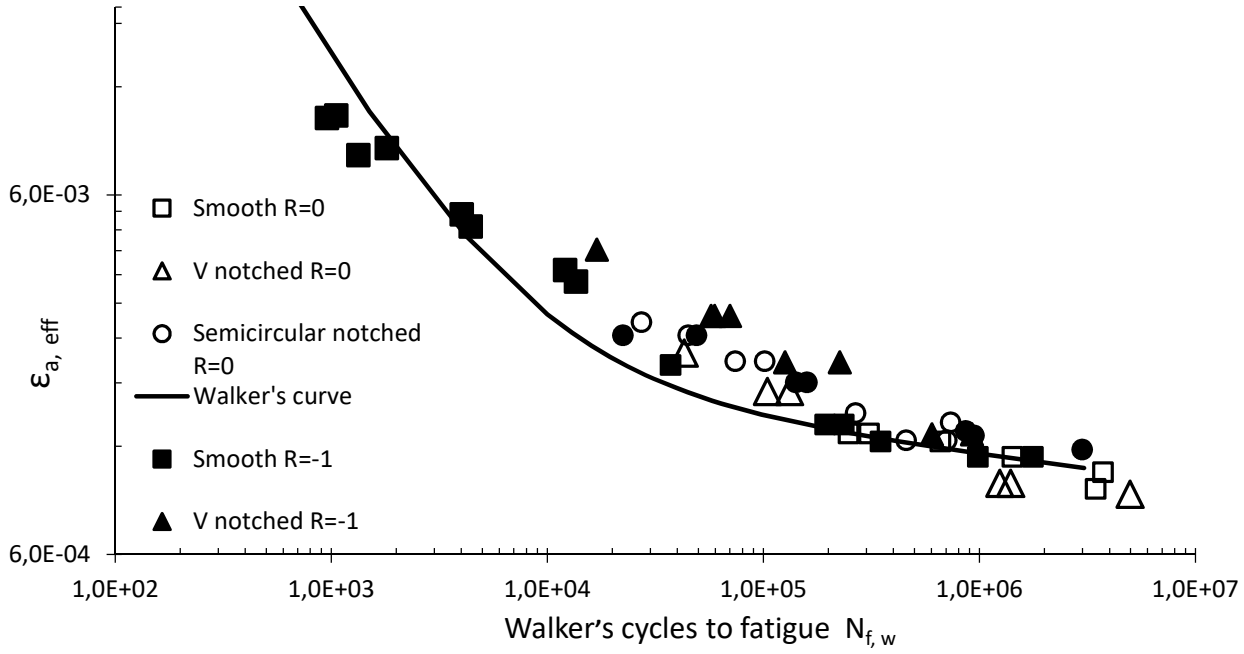

Figure 12: Walker's cycle fatigue against effective strain amplitude for axisymmetric specimens

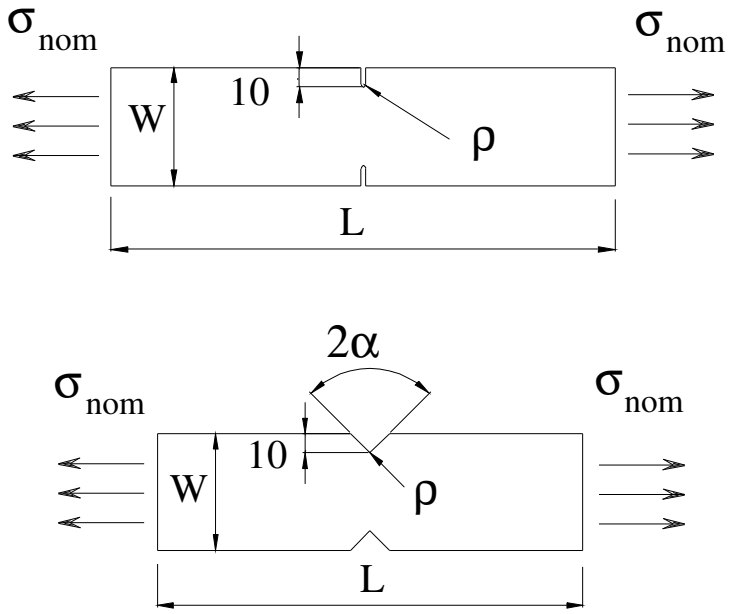

Figure 13: Geometry of specimens made of FeP04 deep drawing steel [22] (W=60 mm, L= 220 mm, thickness 2 mm)

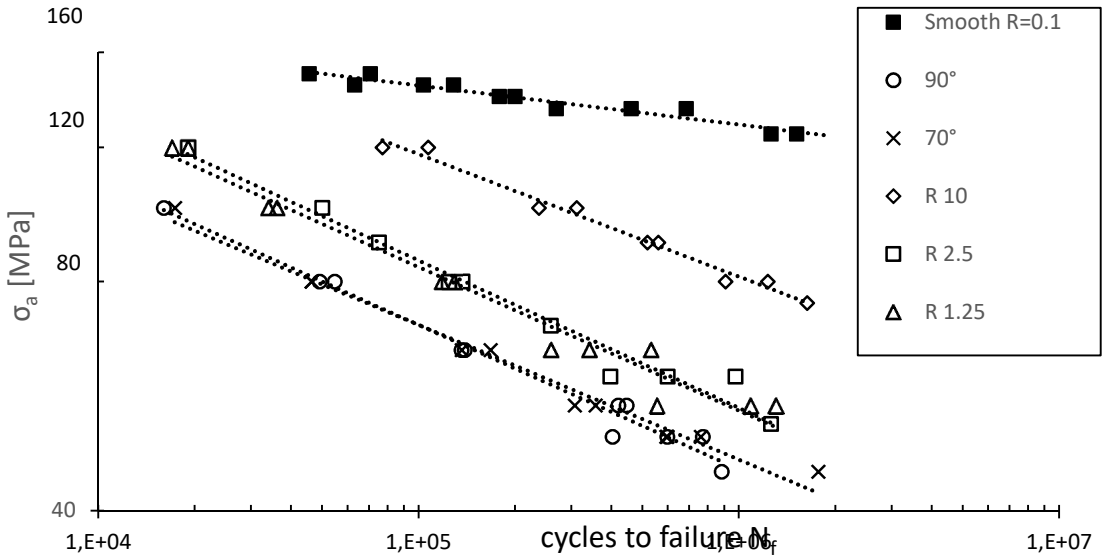

Figure 14: Nominal stress to net section versus cycle fatigue for FeP04 deep drawing steel [22]

(nominal load ratio R=0.1 for all specimens)

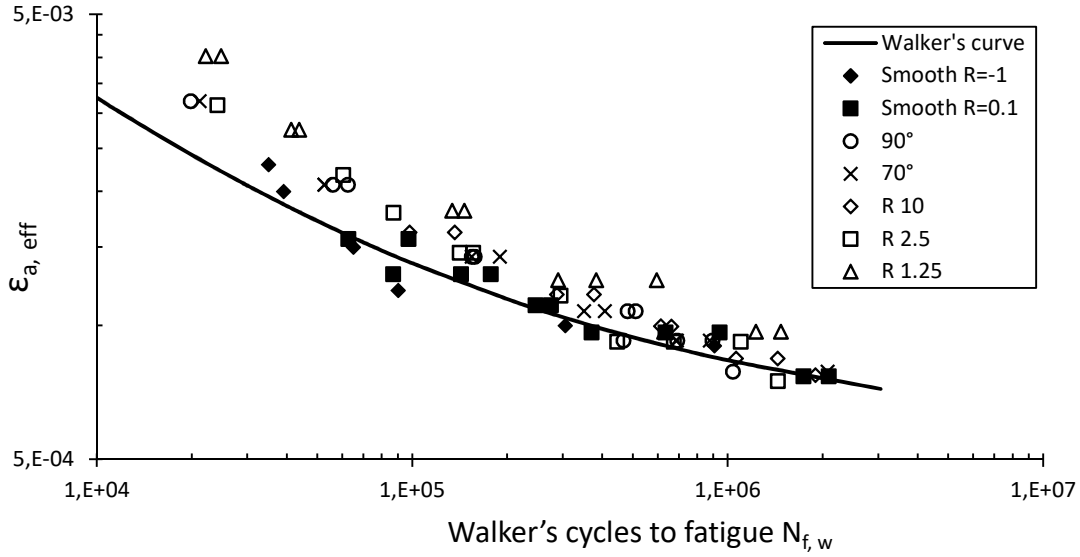

Figure 15: Effective strain amplitude evaluated with gradient approach versus the fatigue Walker's life parameter